water

MDPI

Article

Dual-Frequency Ultrasonic Inactivation of *Escherichia coli* and *Enterococcus faecalis* Using Persulfate: A Synergistic Effect

Natalia Garkusheva [1], Irina Tsenter [1], Elena Kobunova [2], Galina Matafonova [1,*] and Valeriy Batoev [1]

[1] Laboratory of Engineering Ecology, Baikal Institute of Nature Management SB RAS, 670047 Ulan-Ude, Russia
[2] Chemistry Department, Buryat State University, 670000 Ulan-Ude, Russia
* Correspondence: ngal@binm.ru

Abstract: Dual-frequency ultrasound (DFUS) has received considerable attention for enhanced inactivation of microbial pathogens for medical treatment, but remains little investigated for water disinfection. This study is focused on inactivation of *E. coli* and *E. faecalis* in aqueous solution under dual-frequency ultrasonication at 120 + 1700 kHz using persulfate. Single-frequency ultrasonic inactivation showed the higher efficiency of 1700 kHz, compared to 120 kHz. Under the experimental conditions used, no measurable synergy between two frequencies was observed in the absence of persulfate. A high time-based synergistic effect in terms of total inactivation (5-log) of both bacterial species was achieved by DFUS-activated persulfate with synergistic indices of 1.8–5.0. We assume that this is attributed to increased generation of reactive oxygen species (primarily, sulfate anion ($SO_4\bullet^-$) and hydroxyl (•OH) radicals) as a result of enhanced acoustic cavitation. Radical probing and scavenging tests confirmed the generation of radicals and showed a nearly equal contribution of •OH and $SO_4\bullet^-$. This method could be an attractive alternative to ultraviolet technology for fast and effective water disinfection.

Keywords: dual-frequency ultrasound; high frequency; 1.7 MHz; 120 kHz; synergistic effect; persulfate; inactivation; water disinfection

Citation: Garkusheva, N.; Tsenter, I.; Kobunova, E.; Matafonova, G.; Batoev, V. Dual-Frequency Ultrasonic Inactivation of *Escherichia coli* and *Enterococcus faecalis* Using Persulfate: A Synergistic Effect. *Water* **2022**, *14*, 2604. https://doi.org/10.3390/w14172604

Academic Editors: Yulin Tang and Cheng Liu

Received: 14 July 2022
Accepted: 20 August 2022
Published: 24 August 2022

1. Introduction

To date, the World Health Organization (WHO) estimates that at least 2 billion people use microbially contaminated sources of drinking water, which transmits diseases, such as diarrhea and dysentery, and causes 485,000 diarrheal deaths each year [1]. Reducing the level of microbial pathogens in water bodies is essentially important for the protection of drinking water quality and public health. Ultrasonication is regarded as an effective reagent-free method of water disinfection, which is much less affected by water quality compared to ultraviolet technology [2]. It is known that the ultrasonic acoustic wave of sufficient power causes cavitation, which produces collapsing microbubbles in water. This leads to generation of reactive oxygen species (ROS), such as hydroxyl radicals (•OH), which are responsible for inactivation processes [3]. Cavitation also induces different mechanical effects, which in addition damage the cell [4–6]. A synergistic effect is achievable under irradiation of water with two ultrasonic frequencies. In this regard, dual-frequency ultrasound (DFUS) has received considerable attention for water treatment and the related research has been recently reviewed [7]. The literature survey showed that microbial inactivation in water by DFUS remained much less investigated, compared to degradation of organic pollutants. In related research, only low frequencies (≤100 kHz) were used in combinations of 16 + 20 kHz [8], 17 + 33 and 70 + 100 kHz, coupled with NaClO [9,10]. A high-frequency ultrasound above 100 kHz and in the megahertz range has not been used in dual combinations for water disinfection so far. Meanwhile, high frequencies were successfully applied for medical treatment (sonodynamic therapy). In general, it is based on the apoptosis of pathogenic cells (e.g., cancer cells) by ROS, which are produced upon

activation of sonosensitizers with frequencies up to 2 MHz, including DFUS [11,12]. For instance, the synergistically enhanced •OH generation was reported earlier in sonodynamic therapy under exposure to DFUS at 0.5 + 1 MHz and TiO_2 [13]. In view of this, DFUS-based advanced oxidation processes (AOPs) using high frequencies can be identified as an emerging research field and a promising tool for water disinfection.

Among environmentally safe oxidants (hydrogen peroxide, permanganate, ferrate), persulfate (PS) has been extensively employed in sulfate radical (SR)-based AOPs for water treatment and disinfection [14–17]. Its oxidation potential (E_0 = 2.07 V) is higher than permanganate (E_0 = 1.7 V) and hydrogen peroxide (E_0 = 1.77 V) [18]. Due to their higher stability, PS salts are easily transported, stored and dosed. It is activated by many methods, including acoustic cavitation, via homolysis of the O-O bond and production of sulfate radicals (1). •OH are further generated upon their reaction with water (2):

$$S_2O_8^{2-} \xrightarrow{)))} 2SO_4\bullet^- \quad (1)$$

$$SO_4\bullet^- + H_2O \rightarrow \bullet OH + HSO_4^- \quad (2)$$

Accordingly, the higher radical yield is achievable in SR-AOPs. The main advantages of $SO_4\bullet^-$ over •OH include higher redox potential (E_0 = 2.6–3.1 V versus 1.9–2.7 V) [19], a longer half-life and a wider range of operational parameters (e.g., pH) [20,21].

The efficiency of radicals' generation also depends on the ultrasonic frequency. Wang and Wang (2022) [18] concluded that, with increasing frequency, cavitation promotes the conversion of PS and more radicals are generated. Earlier, Kermani et al. (2020) [22] found that furfural degradation by sono-activated PS after 90 min exposure increased from 50.6 to 95.3% by increasing the frequency from 35 to 130 kHz. Therefore, in view of increased ROS production and intensification of inactivation processes, high-frequency ultrasound represents an attractive alternative to low-frequency ultrasound in PS-based processes. To date, there have been only a few reports on microbial inactivation by sono-activated PS at 35 kHz [23] and 600 kHz [24,25] involving iron-catalyzed processes. At the time of writing, no more studies have been published with a focus on water disinfection by DFUS-activated PS, as well as by DFUS alone, at high frequencies above 100 kHz. In our previous studies, a single frequency of 1700 kHz was applied for intensifying bacterial inactivation by sonophotolysis [26,27] and sono-photo-Fenton-like process [28].

The aim of the present study was to evaluate a synergistic effect of dual-frequency ultrasound on inactivating *Escherichia coli* and *Enterococcus faecalis* in model aqueous solution using persulfate. The generation of radicals and the mechanisms of synergistic inactivation, which are based on increased ROS yield and sonoporation due to the generation of additional frequencies under DFUS exposure, have been also considered. This work is the first application of high frequencies in dual combination of 120 + 1700 kHz for water disinfection purposes. These frequencies were selected due to the availability of cheap commercial transducers and generators, which makes their practical application technically and economically feasible. The frequency of 120 kHz is used for fine cleaning of complex parts in industry, whereas 1700 kHz is widely applied for creating water mist and humidifying the air.

2. Materials and Methods

The strains of *Escherichia coli* K-12 and *Enterococcus faecalis* B 4053 were purchased from All-Russian collection of industrial microorganisms (Genetika, Moscow, Russia) and used as indicators of fecal contamination in water. Overnight cultures of *E. coli* and *E. faecalis* were obtained by aerobic incubation of lyophilized cells (37 °C, 180 rpm) in nutrient broth (SRCAMB, Obolensk, Russia) and tryptic soy broth (Merck, Kenilworth, USA), respectively. Afterwards, the cells were centrifuged (4000 rpm, 5 min), washed twice with phosphate-buffered saline (PBS) at pH 7.4 (Gibco® Life technologies, Paisley, UK) and resuspended in fresh PBS to obtain the stock bacterial suspension (10^8 CFU/mL). An aliquot of 0.15 mL

was added to deionized water (1.5 L) to obtain a synthetic water with an initial population of 10^5 CFU/mL.

Disinfection experiments were conducted in an orthogonal dual-frequency sonoreactor, which represents a rectangular cuboid with a capacity volume of 4 L (Figure 1).

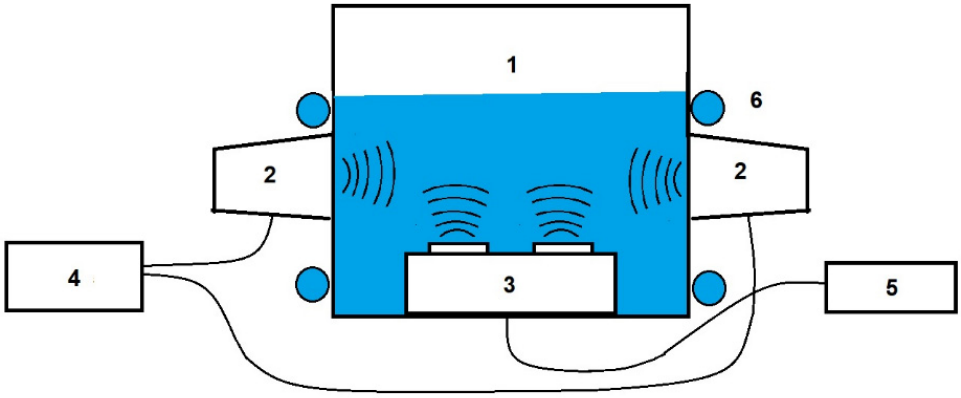

Figure 1. A scheme of a dual-frequency sonoreactor. 1—stainless steel bath, 2—piezoceramic transducer (120 kHz), 3—piezoceramic transducers and generator unit (1700 kHz), 4—ultrasonic generator (120 kHz), 5—power unit (48 V), 6—cooling tubes.

Four piezoceramic transducers (120 kHz, 50 W each, Fan Ying Sonic, Granbosonic Ultrasonic Generator 300 W/120 kHz, Shenzhen, China) were mounted on its long opposite sides (two transducers on each side). Six transducers (1700 kHz, total power 150 W, MSX, model ZCX-RM6D48F, Jiaxing, China) and a generator were assembled into a compact unit and placed on the ground of the reactor to be orthogonally positioned to the 120 kHz transducers. The power unit (Stepperonline, model S-250-48, Nanjing, China) was outside the bath. The temperature of irradiated water was kept at 20 ± 2 °C by circulating cooling water through the copper tubes. Deionized water, artificially contaminated with *E. coli* or *E. faecalis* (10^5 CFU/mL), was irradiated simultaneously with two frequencies in the absence or presence of potassium persulfate (Vekton, St. Petersburg, Russia). Control experiments included irradiation of contaminated water with single frequency at 120 or 1700 kHz. Samples (0.1 mL each) were withdrawn after each exposure, diluted (if required), spread onto nutrient agar (*E. coli*) and tryptic soy agar (*E. faecalis*) plates in triplicate and incubated for 24 h at 37 °C. The survived cells were counted as CFU/mL and plots of the log reduction ($Lg(N/N_0)$) versus exposure time (min) were obtained to monitor the inactivation kinetics. Each experiment was conducted in triplicate and the obtained data were statistically treated using Statistica 10.0 software.

Radical probing experiments were performed in the same sonoreactor using 20 μM *p*-chlorobenzoic acid (*p*CBA, 99%, Acros, Geel, Belgium) as a reference compound. Radical scavenging tests for evaluating the contribution of $SO_4\bullet^-$ and •OH were also conducted using *p*CBA in the presence of methanol and *t*-buthanol (Khimreaktivsnab, Ufa, Russia). Samples after each exposure were analyzed for residual concentration by HPLC (Agilent 1260 Infinity chromatograph, Zorbax SB-C18 column, UV detector). *p*CBA was eluted with a mixture of methanol and 1% acetic acid (70:30) at a flow rate of 0.8 mL/min and detected at 230 nm. Degradation plots were presented as the ratio of residual and initial concentration (C/C_0) versus treatment time (min).

3. Results and Discussion

Figure 2 shows that no measurable inactivation of both bacteria was observed by single-frequency ultrasonication for 60 min. Dual-frequency ultrasonication achieved only ~1-log reduction of *E. coli* and showed no inactivation of *E. faecalis*.

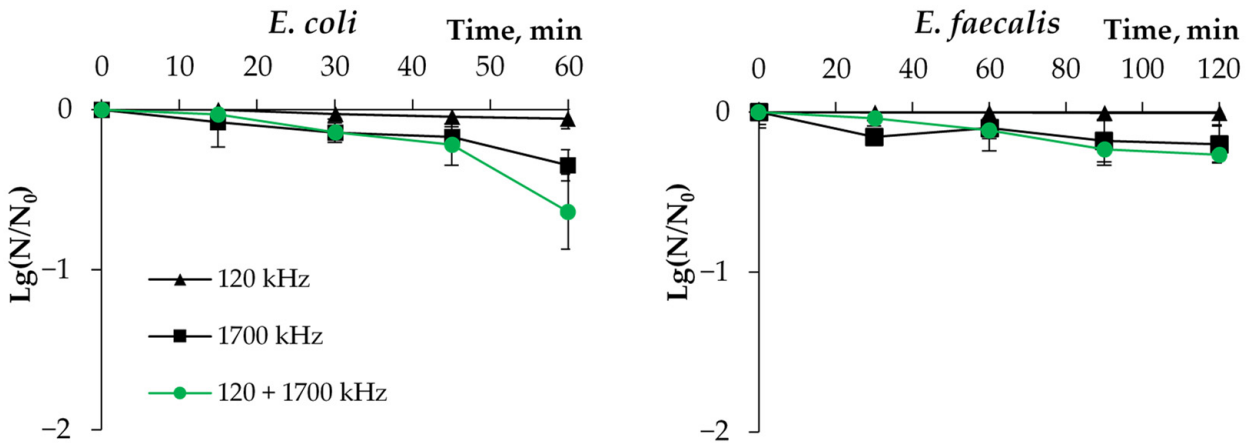

Figure 2. Inactivation of *E. coli* and *E. faecalis* by single- and dual-frequency ultrasound. Error bars represent ±SD.

To enhance ROS generation, further experiments were performed using sono-activated persulfate at initial concentrations of 100 and 200 mg/L [23]. Generally, the gram-positive *E. faecalis* was inactivated markedly slower than the gram-negative *E. coli* due to the thicker peptidoglycan layer (40 nm) of the cell membrane [29]. On increasing the PS concentration, the inactivation rate was expectedly increased due to enhanced ROS production and, accordingly, the treatment time for 5-log reduction (total inactivation) was reduced (Figure 3).

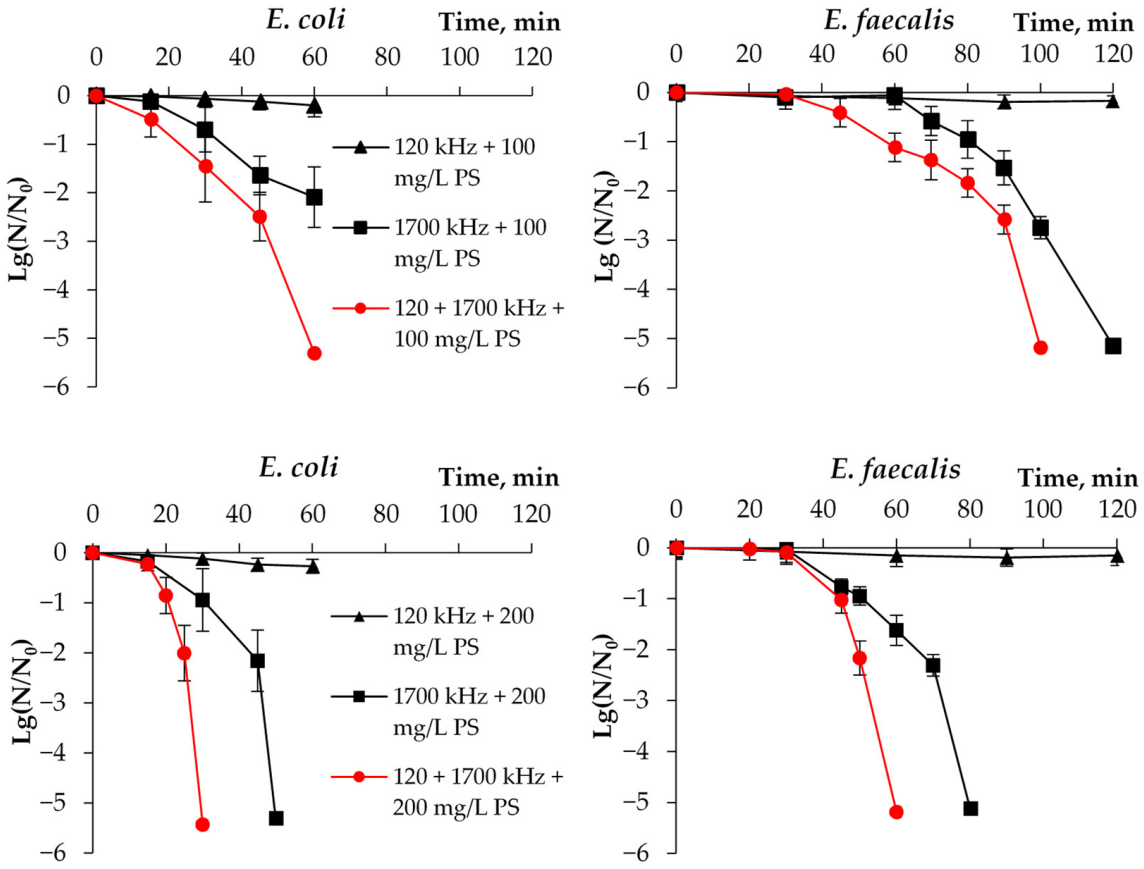

Figure 3. Inactivation of *E. coli* and *E. faecalis* by single- and dual-frequency ultrasound in the presence of persulfate (PS). Error bars represent ±SD.

Comparison of single-frequency inactivation kinetics showed the higher efficiency of 1700 kHz, compared to 120 kHz. This result is consistent with the observation that ROS generation increases with increasing frequency [30]. This dependence is attributed to a decrease of the resonant bubbles' radii at higher frequencies that accelerates their collapse (cavitation). Specifically, Hua and Hoffmann (1997) [31] showed that the bubble radius decreased from 177 μm at 20 kHz to 7 μm at 500 kHz, leading to higher rates of H_2O_2 and •OH production. Our data suggest that PS, activated by 1700 kHz, yields more SO_4•$^-$ and •OH, thereby providing faster inactivation. Radical probing experiments with *p*CBA, which is oxidized by both sulfate and hydroxyl radicals, confirmed this conclusion: its degradation rate was higher at 1700 kHz in the absence and presence of PS (Figure 4). Furthermore, the persulfate-assisted DFUS treatment revealed a synergistically accelerated degradation that indicates the increased generation of radicals. The contribution of •OH from DFUS alone to *p*CBA degradation was estimated to be 35% (Figure 4a).

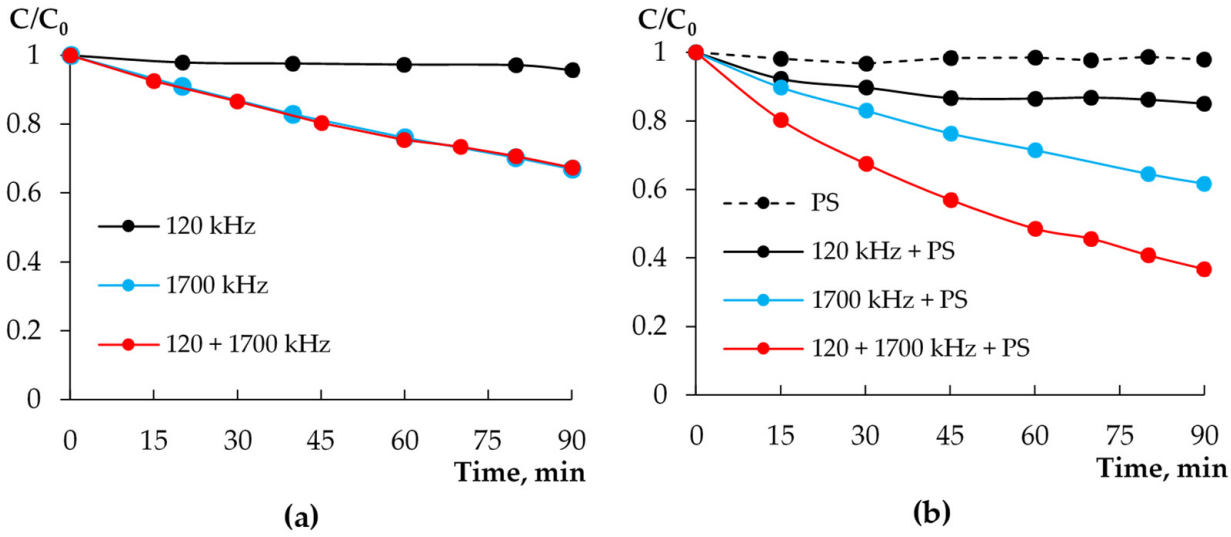

Figure 4. *p*CBA degradation by single- and dual-frequency ultrasound in the absence (**a**) and presence of persulfate (**b**). $[pCBA]_0$ = 20 μM, $[PS]_0$ = 200 mg/L.

The rate constant for the reaction of *p*CBA with SO_4•$^-$ ($k_{pCBA/SO4•-}$ = 3.6 × 10^8 M^{-1} s^{-1} [32]) is only one order of magnitude lower than that with •OH ($k_{pCBA,•OH}$ = 5 × 10^9 M^{-1} s^{-1} [33]). Therefore, it is difficult to distinguish between •OH and SO_4•$^-$ from the obtained degradation plots. To evaluate the contribution of •O H and SO_4•$^-$, *p*CBA was degraded in the presence of *t*-buthanol ($k_{SO4•^-}$ = 4.0 × 10^5 M^{-1} s^{-1}, $k_{OH•}$ = 6.0 × 10^8 M^{-1} s^{-1}) and methanol ($k_{SO4•^-}$ = 1.1 × 10^7 M^{-1} s^{-1}, $k_{OH•}$ = 9.7 × 10^8 M^{-1} s^{-1}) as radical scavengers [34–36]. Importantly, *t*-buthanol reacts with •OH by ~10^3 orders of magnitude faster than with SO_4•$^-$. Alcohols were added individually to *p*CBA solution to obtain a molar ratio of 100:1 (alcohol:persulfate) and sufficiently quench the radicals.

Figure 5 shows that both alcohols inhibited the degradation: methanol scavenged both radicals and *t*-buthanol scavenged primarily •OH.

Assuming that *p*CBA was degraded by SO_4•$^-$ in the presence of *t*-buthanol (which scavenges •OH), the contribution of •OH can be obtained as the arithmetical difference between the degradation efficiency with *t*-buthanol (29%) and without both scavengers (63%) [37,38]. Accordingly, •OH (34%) and SO_4•$^-$ (29%) nearly equally contributed to *p*CBA degradation for 90 min. Such a relatively high •OH yield might be attributed to the additional contribution of 1700 kHz (Figure 4a). It should be emphasized that ROS generation upon sono-activation of PS has been little investigated; however, SO_4•$^-$ rather than •OH was reported to be the predominant radical under exposure to low frequency at 28 kHz [39]. Our study showed that the frequency of 120 kHz is less effective than 1700 kHz for activating PS and producing radicals. This finding is also supported by

Kumar et al. (2011) [40], who reported faster inactivation at 130 kHz than at 35 kHz, which implies the increased radical generation at higher frequency.

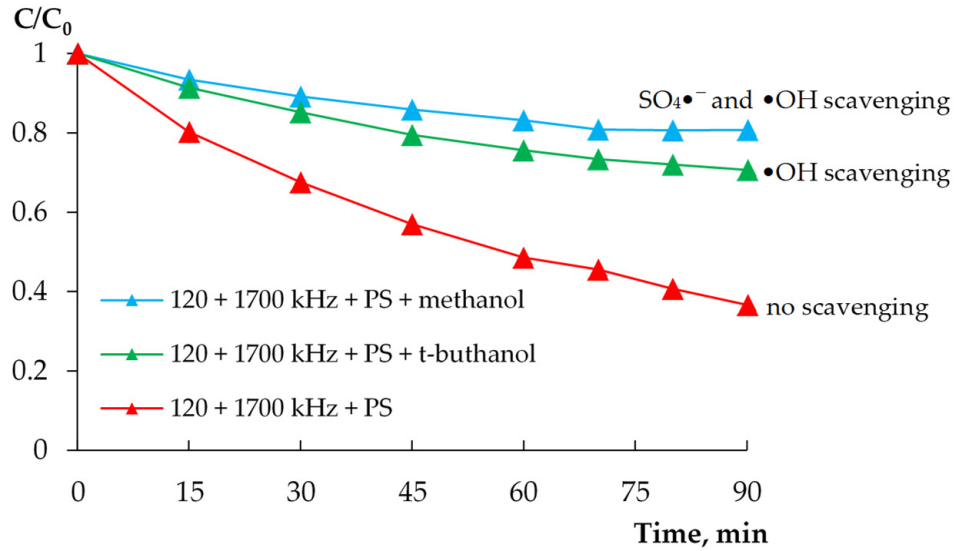

Figure 5. *p*CBA degradation by dual-frequency ultrasound in the presence of alcohols. $[pCBA]_0$ = 20 μM, $[PS]_0$ = 200 mg/L (0.74 mM), $[alcohol]_0$ = 74 mM.

Another possible mechanism of inactivation is sonoporation, which represents the cell permeabilization by acoustic cavitation during ultrasonic exposure [41]. Since this phenomenon is attractive in view of non-invasive delivery of drugs and genes into cells, sonoporation has been well studied for high frequencies and applied for therapeutic purposes [42,43]. Briefly, during acoustic cavitation the collapsing microbubbles induce shear stress, which results in different biological effects, including production of pores on cells [41,44,45]. The higher the ultrasonic frequency in the range of 0.5–2 MHz, the higher the shear stress and sonoporation [46]. Specifically, the sonoporation increased with efficiencies of 39.5 ± 13.7, 46.6 ± 3.28 and 66.8 ± 5.5% at 1, 2.5 and 5 MHz, respectively [43]. It was also reported that, under ultrasonication at 1.5 MHz, the sonoporation occurs prior to ROS generation [47]. In turn, the increased membrane permeability allows the transfer of ROS (primarily, $SO_4\bullet^-$) through the pores into the cell, leading to its apoptosis. This mechanism explains the higher efficiency of 1700 kHz towards inactivation.

As shown in Figure 3, a high time-based synergistic effect was found under simultaneous dual-frequency ultrasonication (120 + 1700 kHz), which provided much faster total inactivation (5-log reduction), compared to the single-frequency mode. In inactivation studies, a synergistic effect occurs if log reduction after integrated (hybrid) exposure is higher than the algebraic sum of log reductions obtained after individual exposure. A synergistic effect is normally quantified with the synergistic index (φ), which should be above 1; otherwise, an additive (φ = 1) or an antagonistic (φ < 1) effect is stated. As shown in our previous study [48], 5-log reduction was the most representative parameter for assessing the synergistic effect under dual-wavelength ultraviolet treatment. In the present study, a synergistic index was also calculated in terms of 5-log reduction by Formula (3):

$$\varphi = \frac{\text{Log reduction } (120 + 1700 \text{ kHz})}{\text{Log reduction } (120 \text{ kHz}) + \text{ Log reduction } (1700 \text{ kHz})} \quad (3)$$

The log reductions after single-frequency treatment were taken for the same exposure times, at which 5-log reduction in DFUS mode was achieved. The obtained values > 1 indicate a high synergistic effect for inactivation of *E. coli* and *E. faecalis* by persulfate activated by DFUS (Table 1). Increasing the concentration of PS to 200 mg/L increased the synergistic index and enhanced the synergistic effect.

Table 1. The synergistic indices (φ) of inactivation under dual-frequency ultrasonication (120 + 1700 kHz) using persulfate.

Persulfate, mg/L	Sum of Log Reductions for Single-Frequency (Exposure Time)	φ
	E. coli	
100	2.3 (60 min)	2.3
200	1.1 (30 min)	5.0
	E. faecalis	
100	2.9 (100 min)	1.8
200	1.8 (60 min)	2.9

The general mechanism of synergistic effect under DFUS exposure was elucidated in our review [7]. Under single-frequency exposure, the nonlinear dynamics of oscillating microbubbles produces additional acoustic waves at different frequencies, such as harmonics [49], subharmonics [50] and ultraharmonics [51]. Under dual-frequency exposure, i.e., interaction of two acoustic waves at different frequencies, new (combination) frequencies are generated in addition to the main frequencies and accompanying harmonics, subharmonics and ultraharmonics [52]. The combination frequencies represent an algebraic sum or a difference of two main frequencies, main frequencies and harmonics, and so on. Notably, the power of acoustic waves of the sum and the difference of main frequencies is lower only by an order of magnitude than the power of main frequencies [53]. Later, Ye et al. (2019) [54] advanced the theoretical insight into the enhanced acoustic cavitation under dual-frequency exposure and found that the oscillation of cavitational microbubbles becomes more unstable and easier to collapse in the dual-frequency ultrasonic field. The authors also conclude that DFUS can destroy the stable oscillation and accelerate the collapse of microbubbles. In this regard, we propose that this phenomenon results in an increase of ROS yield, thereby intensifying inactivation processes and providing a synergistic effect. A synergistic effect in terms of accelerated inactivation is the main advantage of the proposed method. In view of cost efficiency, modern transducers and generators of high-frequency ultrasound, as well as persulfate, are low-cost and commercially available products. We assume that additional costs associated with using the second frequency, are coverable by significant reduction of treatment time (synergy). Although real water has not been examined in this study, a high synergy can make this method applicable for disinfecting drinking water and scaling up under flow-through conditions. Since ultrasonic waves propagate well in water with suspended particles and coloration, dual-frequency ultrasonication at 120 + 1700 kHz could be also a viable option for disinfecting wastewater.

4. Conclusions

A high time-based synergistic effect in terms of 5-log (total) inactivation of *E. coli* and *E. faecalis* in model aqueous solution was found using dual-frequency ultrasonication at 120 + 1700 kHz in the presence of persulfate. We presume that it is primarily caused by generation of additional frequencies, which, in turn, increase the sonoporation and ROS yield upon activation of persulfate. Comparing single frequencies, 1700 kHz was found to be more efficient than 120 kHz due to enhanced ROS generation. Radical probing showed the accelerated degradation of *p*CBA as a reference compound and confirmed this conclusion. This study demonstrates promising results for fast and environmentally safe disinfection of real waters, including drinking water.

Author Contributions: Investigation, formal analysis and validation, N.G., I.T., E.K.; Methodology, data curation and writing—original draft preparation, G.M.; Conceptualization, project administration, methodology, supervision and writing—review and editing, V.B. All authors have read and agreed to the published version of the manuscript.

Funding: This research was funded by Russian Science Foundation, grant number 22-24-00482.

Institutional Review Board Statement: Not applicable.

Informed Consent Statement: Not applicable.

Data Availability Statement: Not applicable.

Conflicts of Interest: The authors declare no conflict of interest.

References

1. World Health Organization. Drinking Water, Key Facts. Available online: https://www.who.int/news-room/fact-sheets/detail/drinking-water (accessed on 13 July 2022).
2. Joyce, E.M.; Mason, T.J. Sonication used as a biocide. A review: Ultrasound a greener alternative to chemical biocides? *Chim. Oggi Chem. Today* **2008**, *26*, 22–26.
3. Phull, S.S.; Newman, A.P.; Lorimer, J.P.; Pollet, B.; Mason, T.J. The development and evaluation of ultrasound in the biocidal treatment of water. *Ultrason. Sonochem.* **1997**, *4*, 157–164. [CrossRef]
4. Jyoti, K.K.; Pandit, A.B. Water disinfection by acoustic and hydrodynamic cavitation. *Biochem. Eng. J.* **2001**, *7*, 201–212. [CrossRef]
5. Ananta, E.; Voigt, D.; Zenker, M.; Heinz, V.; Knorr, D. Cellular injuries upon exposure of *Escherichia coli* and *Lactobacillus rhamnosus* to high-intensity ultrasound. *J. Appl. Microbiol.* **2005**, *99*, 271–278. [CrossRef]
6. Gao, S.; Hemar, Y.; Ashokkumar, M.; Paturel, S.; Lewis, G.D. Inactivation of bacteria and yeast using high frequency ultrasound treatment. *Water Res.* **2014**, *60*, 93–104. [CrossRef]
7. Matafonova, G.; Batoev, V. Dual-frequency ultrasound: Strengths and shortcomings to water treatment and disinfection. *Water Res.* **2020**, *182*, 116016. [CrossRef]
8. Wu, X.; Mason, T.J. Evaluation of power ultrasonic effects on algae cells at a small pilot scale. *Water* **2017**, *9*, 470. [CrossRef]
9. Zou, H.; Wang, L. The disinfection effect of a novel continuous-flow water sterilizing system coupling dual-frequency ultrasound with sodium hypochlorite in pilot scale. *Ultrason. Sonochem.* **2017**, *36*, 246–252. [CrossRef]
10. Zou, H.; Tang, H. Comparison of different bacteria inactivation by a novel continuous-flow ultrasound/chlorination water treatment system in a pilot scale. *Water* **2019**, *11*, 258. [CrossRef]
11. Rengeng, L.; Qianyu, Z.; Yuehong, L.; Zhongzhong, P.; Libo, L. Sonodynamic therapy, a treatment developing from photodynamic therapy. *Photodiagn. Photodyn. Ther.* **2017**, *19*, 159–166. [CrossRef]
12. Tabatabaei, Z.S.; Rajabi, O.; Nassirli, H.; Noghreiyan, A.V.; Sazgarnia, A. A comparative study on generating hydroxyl radicals by single and two-frequency ultrasound with gold nanoparticles and protoporphyrin IX. *Australas. Phys. Eng. Sci. Med.* **2019**, *42*, 1039–1047. [CrossRef] [PubMed]
13. Ninomiya, K.; Noda, K.; Ogino, C.; Kuroda, S.; Shimizu, N. Enhanced OH radical generation by dual-frequency ultrasound with TiO_2 nanoparticles: Its application to targeted sonodynamic therapy. *Ultrason. Sonochem.* **2014**, *21*, 289–294. [CrossRef] [PubMed]
14. Guerra-Rodríguez, S.; Rodríguez, E.; Singh, D.N.; Rodríguez-Chueca, J. Assessment of sulfate radical-based advanced oxidation processes for water and wastewater treatment: A review. *Water* **2018**, *10*, 1828. [CrossRef]
15. Xiao, R.; Liu, K.; Lu, B.; Minakata, D.; Seo, Y.; Göktaş, R.K.; Dionysiou, D.D.; Tang, C.-J.; Wei, Z.; Spinney, R. Inactivation of pathogenic microorganisms by sulfate radical: Present and future. *Chem. Eng. J.* **2019**, *371*, 222–232. [CrossRef]
16. Xia, X.; Zhu, F.; Li, J.; Yang, H.; Wei, L.; Li, Q.; Jiang, J.; Zhang, G.; Zhao, Q. A review study on sulfate-radical-based advanced oxidation processes for domestic/industrial wastewater treatment: Degradation, efficiency, and mechanism. *Front. Chem.* **2020**, *8*, 592056. [CrossRef]
17. Giannakis, S.; Lin, A.K.-Y.; Ghanbari, F. A review of the recent advances on the treatment of industrial wastewaters by sulfate radical-based advanced oxidation processes (SR-AOPs). *Chem. Eng. J.* **2021**, *406*, 127083. [CrossRef]
18. Wang, B.; Wang, Y. A comprehensive review on persulfate activation treatment of wastewater. *Sci. Tot. Environ.* **2022**, *831*, 154906. [CrossRef]
19. Oh, W.-D.; Dong, Z.; Lim, T.-T. Generation of sulfate radical through heterogeneous catalysis for organic contaminants removal: Current development, challenges and prospects. *Appl. Catal. B* **2016**, *194*, 169–201. [CrossRef]
20. Yang, Q.; Ma, Y.; Chen, F.; Yao, F.; Sun, J.; Wang, S.; Yi, K.; Hou, L.; Li, X.; Wang, D. Recent advances in photo-activated sulfate radical-advanced oxidation process (SR-AOP) for refractory organic pollutants removal in water. *Chem. Eng. J.* **2019**, *378*, 122149. [CrossRef]
21. Lee, J.; von Gunten, U.; Kim, J.-H. Persulfate-based advanced oxidation: Critical assessment of opportunities and roadblocks. *Environ. Sci. Technol.* **2020**, *54*, 3064−3081. [CrossRef]
22. Kermani, M.; Farzadkia, M.; Morovati, M.; Taghavi, M.; Fallahizadeh, S.; Khaksefidi, R.; Norzaee, S. Degradation of furfural in aqueous solution using activated persulfate and peroxymonosulfate by ultrasound irradiation. *J. Environ. Manag.* **2020**, *266*, 110616. [CrossRef] [PubMed]
23. Venieri, D.; Karapa, A.; Panagiotopoulou, M.; Gounaki, I. Application of activated persulfate for the inactivation of fecal bacterial indicators in water. *J. Environ. Manag.* **2020**, *261*, 110223. [CrossRef] [PubMed]
24. Wu, X.; Xu, G.; Zhu, J.-J. Sonochemical synthesis of Fe_3O_4/carbon nanotubes using low frequency ultrasonic devices and their performance for heterogeneous sono-persulfate process on inactivation of *Microcystis aeruginosa*. *Ultrason. Sonochem.* **2019**, *58*, 104634. [CrossRef] [PubMed]

25. Wu, X.; Yan, L.; Xu, G.; Wang, X.; Wang, J.J.; Dionysios, D.D. High frequency ultrasonication enhances iron-catalyzed sulphate inactivation of *Escherichia coli* and *Staphylococcus aureus*. *Chem. Eng. J. Adv.* **2021**, *8*, 100170. [CrossRef]
26. Tsenter, I.M.; Matafonova, G.G.; Batoev, V.B. Combination of high frequency ultrasound and UV radiation of excilamp for surface disinfection. *Eng. Life Sci.* **2015**, *15*, 830–834. [CrossRef]
27. Tsenter, I.; Popova, S.; Garkusheva, N. Efficiency of sonophotolysis for eliminating bisphenol A and bacteria from aqueous solution. *IOP Conf. Ser. Mater. Sci. Eng.* **2020**, *962*, 042084. [CrossRef]
28. Popova, S.; Tsenter, I.; Garkusheva, N.; Beck, S.; Matafonova, G.; Batoev, V. Evaluating (sono)-photo-Fenton-like processes with high-frequency ultrasound and UVA LEDs for degradation of organic micropollutants and inactivation of bacteria separately and simultaneously. *J. Environ. Chem. Eng.* **2021**, *9*, 105249. [CrossRef]
29. Chang, J.D.; Wallace, A.G.; Foster, E.E.; Kim, S.J. Peptidoglycan compositional analysis of *Enterococcus faecalis* biofilm by stable isotope labeling by amino acids in bacterial culture. *Biochemistry* **2018**, *57*, 1274–1283. [CrossRef]
30. Mason, T.J.; Cobley, A.J.; Graves, J.E.; Morgan, D. New evidence for the inverse dependence of mechanical and chemical effects on the frequency of ultrasound. *Ultrason. Sonochem.* **2011**, *18*, 226–230. [CrossRef]
31. Hua, I.; Hoffmann, M.R. Optimization of ultrasonic irradiation as an advanced oxidation technology. *Environ. Sci. Technol.* **1997**, *31*, 2237–2243. [CrossRef]
32. Neta, P.; Madhavan, V.; Zemel, H.; Fessenden, R.W. Rate constants and mechanism of reaction of sulfate radical anion with aromatic compounds. *J. Am. Chem. Soc.* **1977**, *99*, 163–164. [CrossRef]
33. Elovitz, M.S.; von Gunten, U. Hydroxyl radical/ozone ratios during ozonation processes. I. The R_{ct} concept. *Ozone Sci. Eng.* **1999**, *21*, 239–260. [CrossRef]
34. Eibenberger, H.; Steenken, S.; O'Neill, P.; Schulte-Frohlinde, D. Pulse radiolysis and electron spin resonance studies concerning the reaction of $SO_4 \cdot^-$ with alcohols and ethers in aqueous solution. *J. Phys. Chem.* **1978**, *82*, 749−750. [CrossRef]
35. Neta, P.; Huie, R.E.; Ross, A.B. Rate constants for reactions of inorganic radicals in aqueous solution. *J. Phys. Chem. Ref. Data* **1988**, *17*, 1027–1284. [CrossRef]
36. Buxton, G.V.; Greenstock, C.L.; Helman, W.P.; Ross, A.B. Critical review of rate constants for reactions of hydrated electrones, hydrogen atoms and hydroxyl radicals (•OH/•O^-) in aqueous solution. *J. Phys. Chem. Ref. Data* **1988**, *17*, 513–886. [CrossRef]
37. Michael-Kordatou, I.; Iacovou, M.; Frontistis, Z.; Hapeshi, E.; Dionysiou, D.D.; Fatta-Kassinos, D. Erythromycin oxidation and ERY-resistant *Escherichia coli* inactivation in urban wastewater by sulfate radical-based oxidation process under UV-C irradiation. *Water Res.* **2015**, *85*, 346–358. [CrossRef]
38. Popova, S.; Matafonova, G.; Batoev, V. Simultaneous atrazine degradation and *E. coli* inactivation by UV/$S_2O_8^{2-}$/Fe^{2+} process under KrCl excilamp (222 nm) irradiation. *Ecotoxicol. Environ. Saf.* **2019**, *169*, 169–177. [CrossRef]
39. Lu, X.; Zhao, J.; Wang, Q.; Wang, D.; Xu, H.; Ma, J.; Qiu, W.; Hu, T. Sonolytic degradation of bisphenol S: Effect of dissolved oxygen and peroxydisulfate, oxidation products and acute toxicity. *Water Res.* **2019**, *165*, 114969. [CrossRef]
40. Kumar, R.; Yadav, N.; Rawat, L.; Goyal, M.K. Effect of two waves of ultrasonic on waste water treatment. *J. Chem. Eng. Process Technol.* **2014**, *5*, 1000193.
41. Lentacker, I.; De Cock, I.; Deckers, R.; De Smedt, S.C.; Moonen, C.T.W. Understanding ultrasound induced sonoporation: Definitions and underlying mechanisms. *Adv. Drug Deliv. Rev.* **2014**, *72*, 49–64. [CrossRef]
42. Zhou, Y.; Yang, K.; Cui, J.; Ye, J.Y.; Deng, C.X. Controlled permeation of cell membrane by single bubble acoustic cavitation. *J. Control. Release* **2012**, *157*, 103–111. [CrossRef] [PubMed]
43. Burgess, M.T.; Porter, T.M. Control of acoustic cavitation for efficient sonoporation with phase-shift nanoemulsions. *Ultrasound Med. Biol.* **2019**, *45*, 846–858. [CrossRef] [PubMed]
44. Wu, J. Shear stress in cells generated by ultrasound. *Prog. Biophys. Mol. Biol.* **2007**, *93*, 363–373. [CrossRef]
45. Collis, J.; Manasseh, R.; Liovic, P.; Tho, P.; Ooi, A.; Petkovic-Duran, K.; Zhu, Y. Cavitation microstreaming and stress fields created by microbubbles. *Ultrasonics* **2010**, *50*, 273–279. [CrossRef] [PubMed]
46. Helfield, B.; Chen, X.; Watkins, S.C.; Villanueva, F.S. Biophysical insight into mechanisms of sonoporation. *Proc. Natl. Acad. Sci. USA* **2016**, *113*, 9983–9988. [CrossRef]
47. Jia, C.; Xu, L.; Han, T.; Cai, P.; Yu, A.C.H.; Qin, P. Generation of reactive oxygen species in heterogeneously sonoporated cells by microbubbles with single-pulse ultrasound. *Ultrasound Med. Biol.* **2018**, *44*, 1074–1085. [CrossRef] [PubMed]
48. Tsenter, I.; Garkusheva, N.; Matafonova, G.; Batoev, V. A novel water disinfection method based on dual-wavelength UV radiation of KrCl (222 nm) and XeBr (282 nm) excilamps. *J. Environ. Chem. Eng.* **2022**, *10*, 107537. [CrossRef]
49. Umemura, S.; Kawabata, K.; Sasaki, K. In vitro and in vivo enhancement of sonodynamically active cavitation by second-harmonic superimposition. *J. Acoust. Soc. Am.* **1997**, *101*, 569–577. [CrossRef]
50. Jin, J.; Hayashi, T.; Miwa, T. Observation of noise generation induced in ultrasonic cavitation with ultramicroelectrode. *Chem. Lett.* **1998**, *27*, 539–540. [CrossRef]
51. Petošić, A.; Ivančević, B.; Svilar, D. Measuring derived acoustic power of an ultrasound surgical device in the linear and nonlinear operating modes. *Ultrasonics* **2009**, *49*, 522–531. [CrossRef]
52. Liu, H.; Hsieh, C. Single-transducer dual-frequency ultrasound generation to enhance acoustic cavitation. *Ultrason. Sonochem.* **2009**, *16*, 431–438. [CrossRef] [PubMed]

53. Zhang, Y.; Zhang, Y.; Li, S. Combination and simultaneous resonances of gas bubbles oscillating in liquids under dual-frequency acoustic excitation. *Ultrason. Sonochem.* **2017**, *35*, 431–439. [CrossRef] [PubMed]
54. Ye, L.; Zhu, X.; Liu, Y. Numerical study on dual-frequency ultrasonic enhancing cavitation effect based on bubble dynamic evolution. *Ultrason. Sonochem.* **2019**, *59*, 104744. [CrossRef] [PubMed]